Clustering, Fronts, and Heat Transfer in Turbulent Suspensions of Heavy Particles

Jérémie Bec, Holger Homann, and Giorgio Krstulovic
Laboratoire Lagrange, UMR7293, Université de Nice Sophia-Antipolis, CNRS, Observatoire de la Côte d'Azur, CS 34229, 06304 Nice Cedex 4, France
(Received 9 January 2014; published 13 June 2014)

Heavy inertial particles transported by a turbulent flow are shown to concentrate in the regions where an advected passive scalar, such as temperature, displays very strong frontlike discontinuities. This novel effect is responsible for extremely high levels of fluctuations for the passive field sampled by the particles that impacts the heat fluxes exchanged between the particles and the surrounding fluid. Instantaneous and averaged heat fluxes are shown to follow strongly intermittent statistics and anomalous scaling laws.

DOI: 10.1103/PhysRevLett.112.234503 PACS numbers: 47.27.−i, 47.10.−g, 47.55.Kf

Turbulent transport has the contradictory feature of enhancing the dispersion of passive substances and triggering the clustering of finite-size impurities. These two violent mechanisms are simultaneously at play for the heat exchanges in colloidal nanofluids [1], for the condensation of cloud droplets in a supersaturated environment [2], for the interactions between plankton and nutrients [3], and for the accretion of gas and dust by planetary embryos [4]. As the induced biases are apparently opposite, it is commonly presumed that the dispersed particles sample the field with which they interact in a uniform and uncorrelated manner. Such arguments justify the mean-field kinetic approaches describing the rates at which particles change phase, change size, or multiply. We show in this Letter that the complex dynamic behavior of the carrier turbulent flow concentrates finite-size particles in the regions where the passive scalar displays very strong frontlike discontinuities. This new effect is responsible for extremely high levels of fluctuations for the passive field sampled by the particles and henceforth breaks the underlying assumptions of traditional approaches.

Heavy particles are ejected by inertial centrifugal forces from vortices and form preferential concentrations. Consequently, they sample the underlying flow in a very nonuniform manner. At the same time, passively transported fields develop nontrivial geometrical and statistical properties, displaying anomalous scaling laws [5]. Turbulence creates *fronts* across which the scalar strongly varies on very small length scales [6]. Such quasidiscontinuities appear at the boundaries between the different circulation zones of the flow and concentrate diffusion. Mixing is weakened in preferential concentrations and enhanced in fronts. While these two kinds of inhomogeneities result from turbulent eddies, very little is known on how they relate. To address this issue we consider a passive scalar field θ evolving according to the advection-diffusion equation

$$\partial_t \theta + \boldsymbol{u} \cdot \nabla \theta = \kappa \nabla^2 \theta + \varphi, \tag{1}$$

where $\boldsymbol{u}(\boldsymbol{x}, t)$ is a stationary homogeneous and isotropic turbulent velocity field solving the three-dimensional incompressible Navier-Stokes equation, κ is the diffusivity, and $\varphi(\boldsymbol{x}, t)$ is a large-scale force. In many physical situations, for instance, in clouds or in convection experiments, there is an imposed mean scalar gradient $\boldsymbol{G}$. This gradient, which can be taken into account by setting $\varphi = -\boldsymbol{G} \cdot \boldsymbol{u}$, breaks the isotropy of the system. However, it is known that the scaling properties of a passive scalar are universal and do not depend on the large-scale forcing [7]. Therefore, in this Letter, unless explicitly mentioned, we use a large-scale white noise in time forcing in order to preserve isotropy. At the same time we solve (1), we consider heavy inertial (point) particles which experience a viscous drag with the velocity field $\boldsymbol{u}$. Their individual trajectories are given by

$$\dot{\boldsymbol{X}}_p = \boldsymbol{V}_p, \qquad \dot{\boldsymbol{V}}_p = -\frac{1}{\tau_p}[\boldsymbol{V}_p - \boldsymbol{u}(\boldsymbol{X}_p, t)], \tag{2}$$

where dots designate time derivatives. The relaxation time reads $\tau_p = 2\rho_p a^2/(9\rho_f \nu)$, ρ_p and ρ_f being the particle and fluid mass density, respectively, a the particle radius, and ν the fluid kinematic viscosity. Particle inertia is measured in terms of the Stokes number $\mathrm{St} = \tau_p/\tau_\eta$, where τ_η designates the turnover time associated with the Kolmogorov dissipative scale η (the smallest active scale of the turbulent flow). The case $\mathrm{St} = 0$ corresponds to tracers (inertialess particles), whose dynamics is $\dot{\boldsymbol{X}}_p = \boldsymbol{u}(\boldsymbol{X}_p, t)$.

We make use of direct numerical simulations of the incompressible Navier-Stokes equations with a large-scale forcing. The velocity field $\boldsymbol{u}$ and the advected passive scalar θ are obtained by the (standard) pseudospectral code LaTu [8] using 512^3 and 1024^3 grid points (corresponding to Taylor-scale Reynolds numbers $R_\lambda = 180$ and 315). We consider a scalar field of Schmidt number one ($\kappa = \nu$). The values of the different fields at the particle positions are obtained by tricubic interpolation. The Lagrangian trajectories of millions of particles with different values of the

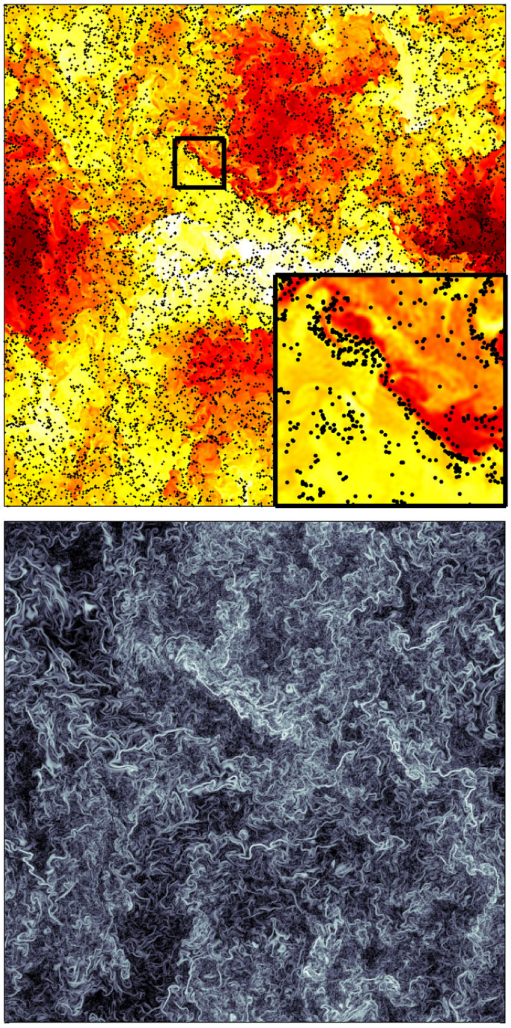

FIG. 1 (color online). Top: snapshot of the scalar field θ (from white to dark red), together with the positions of St $= 1$ particles (black dots) in a thin slice of width $\simeq\eta$ at $R_\lambda \approx 315$. The lower-right inset shows a zoom of the black box. Bottom: corresponding snapshot of the scalar dissipation rate ϵ_θ (from black to white).

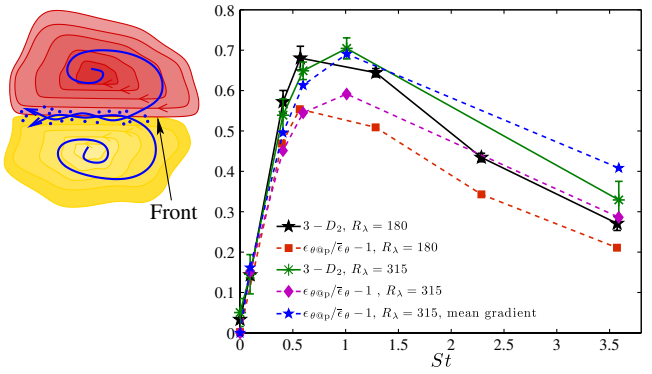

FIG. 2 (color online). Left: sketch of the mechanism leading to the concentration of particles in the fronts of the scalar field. The red and yellow areas outline two different Lagrangian coherent structures and the blue lines show typical particle trajectories. Right: complementary correlation dimension $3 - D_2$ and relative enhancement of the scalar dissipation rate at particle positions $\epsilon_{\theta@p}/\overline{\epsilon_\theta} - 1$ as a function of the Stokes number.

Stokes number St are integrated simultaneously. After a transient, the full system reaches a statistical stationary state and all results of this Letter refer to this regime.

Figure 1 (top) shows a snapshot of the passive scalar field together with particle positions in a thin slice of the three-dimensional domain. The scalar field is characterized by the presence of large-scale regions where it varies smoothly separated by sharp fronts where it varies abruptly. Particles form clusters that display a strong correlation with these fronts as emphasized in the inset. The regions where the scalar is almost constant are the so-called Lagrangian coherent structures of the flow [9]. They relate to zones where the mixing is ineffective and thus consist of fluid elements sharing a common history of the scalar forcing along their paths. Fronts appear at the border between such closed dynamical regions. The inertial centrifugal forces acting on heavy particles are responsible for their ejection from these regions and their concentration at the edges. This mechanism is sketched in Fig. 2 left. The correlations appearing between particle clusters and the fronts of the scalar field certainly relate to the sweep-stick mechanism [10], bringing into question possible relations between the zeros of the fluid acceleration and the strong variations of a passive scalar.

This effect can also be understood by local arguments. The fronts correspond to locations where the scalar dissipation rate $\epsilon_\theta = (\kappa/2)|\nabla\theta|^2$ is very strong. These violent spatial fluctuations are clearly appreciated in Fig. 1 (bottom), where ϵ_θ is displayed for the same snapshot. It is easily seen from (1) that ϵ_θ is stretched by the velocity gradients. Namely, when neglecting the diffusive and forcing terms, the scalar dissipation along tracer trajectories obeys $\dot{\epsilon}_\theta = -\kappa(\nabla\theta)^{\mathsf{T}}\mathbb{S}(\boldsymbol{X}_p, t)\nabla\theta$, where $\mathbb{S}$ is the symmetric part of the fluid velocity gradient tensor $\nabla\boldsymbol{u}$. This results in an enhancement of dissipation in the regions where the fluid flow has a large contraction rate. At the same time, large values of the shear rate $\mathbb{S}$ enhance the concentration of particles. As shown in [11], particles with small inertia (St $\ll 1$) can be approximated as the tracers of a synthetic compressible velocity field, namely, $\dot{\boldsymbol{X}}_p \approx \boldsymbol{v}(\boldsymbol{X}_p, t)$ with $\boldsymbol{v} = \boldsymbol{u} - \tau_p(\partial_t\boldsymbol{u} + \boldsymbol{u}\cdot\nabla\boldsymbol{u})$. For incompressible fluid flows, the divergence of the velocity field $\boldsymbol{v}$ reads $\nabla\cdot\boldsymbol{v} = -\tau_p(\mathrm{tr}\mathbb{S}^2 - |\boldsymbol{\omega}|^2/2)$, where $\boldsymbol{\omega} = \nabla\times\boldsymbol{u}$ is the vorticity. Particles concentrate in high-strain low-vorticity regions, explaining their correlation with the high values of ϵ_θ and the location of the fronts.

A quantitative measurement of particle clustering is given by the correlation dimension D_2, which is estimated by finding the small-scale algebraic behavior of $P_2(r) \sim r^{D_2}$, the probability to find two particles at a distance less than r. The dependence of the codimension $3 - D_2$ on the Stokes number is shown in Fig. 2. A

nonmonotonic behavior with a maximum of clustering at $\mathrm{St} \sim 1$ is observed as in [12]. As particles cluster in the fronts, the average scalar dissipation at the particles' position $\epsilon_{\theta@p}$ is expected to be sensitive to the Stokes number. This is apparent in Fig. 2 where the relative enhancement of the scalar dissipation rate $\epsilon_{\theta@p}/\overline{\epsilon_\theta} - 1$ is also plotted ($\overline{\epsilon_\theta}$ designates here the mean scalar dissipation). The dissipation along particle trajectories can be 70% larger than the average for values of the Stokes number for which preferential concentration is the strongest. Note that this behavior is independent of the way the scalar is forced as it is also observed when an average gradient is imposed.

We now turn to study the statistics of the passive scalar along particles trajectories. It is well known that it presents large fluctuations leading to an anomalous scaling of the Eulerian structure functions [5,6]. Here we focus on the Lagrangian increments of the scalar field $\delta_\tau\theta = \theta(\boldsymbol{X}_p(t+\tau), t+\tau) - \theta(\boldsymbol{X}_p(t), t)$ that strongly depend on the particles' inertia. For $\mathrm{St} = 0$, particles are simple tracers and mainly remain inside the Lagrangian coherent structures. The variations of $\theta(\boldsymbol{X}_p(t))$ are both diffusive due to the forcing φ and relate to the formation, deformation, and destruction of fronts. When $\mathrm{St} > 0$, inertia allows particles to cross the fronts and thus to sample larger fluctuations of the scalar field. When $\mathrm{St} \to \infty$, the particles decouple from the flow and move almost ballistically. A frozen Taylor hypothesis leads then to predict that $\delta_\tau\theta$ is given by the Eulerian increments $\Delta_\ell\theta = \theta(\mathbf{x}+\ell, t) - \theta(\mathbf{x}, t)$ with $\ell \simeq \tau v_p$, where v_p is the typical particle velocity. This is manifest when looking at the moments of the Lagrangian increments that are expected to scale as $\langle|\delta_\tau\theta|^n\rangle \sim \tau^{\zeta_n}$ for $\tau_\eta \ll \tau \ll \tau_L$, with τ_L the large-eddy turnover time of the turbulent flow. Similarly, the Eulerian increments scales as $\langle|\Delta_\ell\theta|^n\rangle \sim \ell^{\zeta_n^E}$ inside the inertial range ($\eta \ll \ell \ll L$ with L the largest scale of the system). Figure 3 shows the scaling exponents ζ_n as a function of their order n for various values of the particle Stokes number St. For tracers ($\mathrm{St} = 0$) the results are very close to the normal scaling $\zeta_n = n/2$, indicating that anomalous corrections, if any, are very weak and quantifying them precisely would require a major augmentation of the statistics. When increasing St the exponents ζ_n go from a tracer behavior to those obtained from Eulerian statistics $\zeta_n = \zeta_n^E$, showing the enhancement of Lagrangian scalar intermittency due to particle inertia.

These findings have important consequences on possible heat exchanges between particles and a carrier fluid. Indeed, let us assume that the transported scalar field is the fluid temperature. For particles much smaller than the scales at which the fluid temperature varies, the heat flux at the particle surface is proportional to the difference between the particle temperature θ_p and that of the environment [13,14], so that

$$\dot{\theta}_p = -\frac{1}{\tau_\theta}[\theta_p - \theta(\boldsymbol{X}_p, t)], \tag{3}$$

where $\tau_\theta = c_p a^2/(3c_f\kappa)$, with c_p and c_f the volumetric heat capacities of the particles and the fluid, respectively. The particles then have a thermal inertia that is measured in terms of the thermal Stokes number $\mathrm{St}_\theta = \tau_\theta/\tau_\eta$.

Heat exchanges between the particles and the fluid are entailed in the dependence of the particle temperature increment $\delta_\tau\theta_p = \theta_p(t+\tau) - \theta_p(t)$ upon the time lag τ. As the system is in a statistical steady state, the increments are independent of t. Different regimes occur. For small time lags $\tau \ll \tau_\theta$, the heat flux remains almost constant and $\theta_p(t+\tau) \simeq \theta_p(t) + \tau\dot{\theta}_p(t)$, so that $\langle\delta_\tau\theta_p^n\rangle \simeq \tau^n\langle\dot{\theta}_p^n\rangle$. This regime is observed in Fig. 4, which represents the evolution of $\langle\delta_\tau\theta_p^2\rangle$ for $\mathrm{St} = 0.6$ and various values of the particle thermal inertia. At larger time lags, one observes that temperature increments follow anomalous scaling laws of the form $\langle\delta_\tau\theta_p^n\rangle \simeq \tau^{\alpha_n}$. This regime occurs when

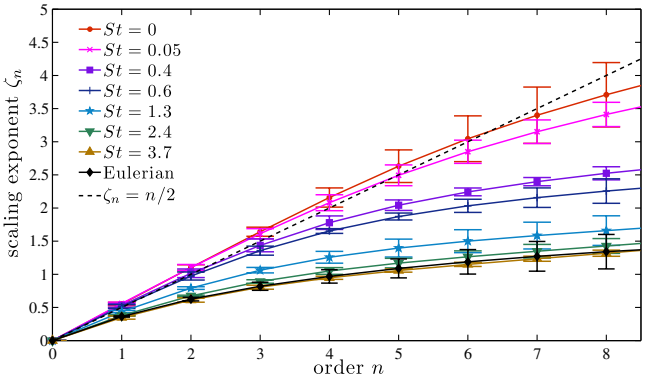

FIG. 3 (color online). Anomalous exponents ζ_n of the Lagrangian increments $\langle|\delta_\tau\theta|^n\rangle \sim \tau^{\zeta_n}$ for different Stokes numbers. The anomalous exponents ζ_n^E of the Eulerian increments $\langle|\Delta_\ell\theta|^n\rangle \sim \ell^{\zeta_n^E}$ are also displayed.

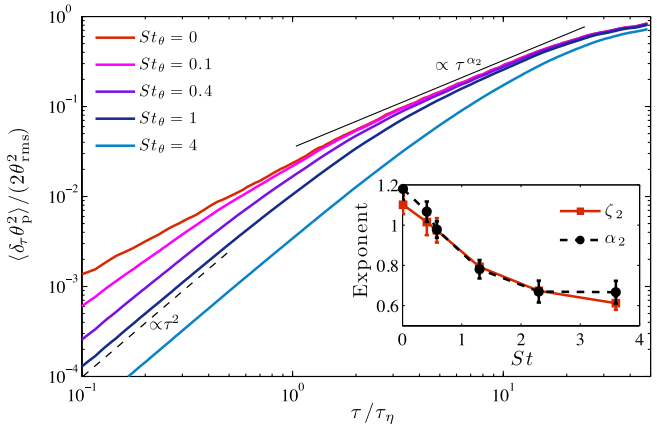

FIG. 4 (color online). Time evolution of $\langle\delta_\tau\theta_p^2\rangle$ for $\mathrm{St} = 0.6$ and five different values of the thermal Stokes number St_θ. The inset displays the exponent α_2 of the inner particle temperature scaling $\delta_\tau\theta_p$ for time lags $\tau \gg \tau_\theta$, together with the anomalous exponent ζ_2 of the fluid temperature for different Stokes numbers.

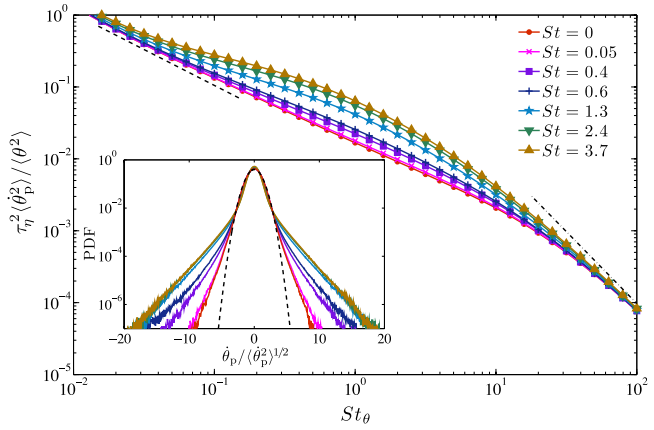

FIG. 5 (color online). Variance of the heat flux $\langle \dot{\theta}_p^2 \rangle$ as a function of the thermal Stokes number St_θ and various particle inertia; the two lines represent the asymptotics $\langle \dot{\theta}_p^2 \rangle \propto \mathrm{St}_\theta^{-1}$ for $\mathrm{St}_\theta \ll 1$ (dashed line) and $\langle \dot{\theta}_p^2 \rangle \propto \mathrm{St}_\theta^{-2}$ for $\mathrm{St}_\theta \gg 1$ (dotted-dashed line). Inset: probability density function (PDF) of the heat flux $\dot{\theta}_\mathrm{p}$ normalized to unit variance for $\mathrm{St}_\theta = 1$ and the different Stokes numbers; the dashed curve shows a Gaussian distribution.

$\tau_\theta \ll \tau \ll \tau_L$ that is in the limit when thermal inertia becomes negligible and particle temperature follows that of the fluid. We then expect $\langle \delta_\tau \theta_p^n \rangle \simeq \langle \delta_\tau \theta^n \rangle$, so that the scaling laws of particle temperature are given by the anomalous Lagrangian exponents of the scalar field introduced above, namely, $\alpha_n = \zeta_n$. This is confirmed from the inset of Fig. 4, where both α_2 and ζ_2 are displayed as a function of the Stokes number.

The instantaneous heat exchanges between the particles and the fluid are also strongly depending on both the thermal and dynamical inertia. This is evidenced from Fig. 5, which represents the heat flux variance $\langle \dot{\theta}_p^2 \rangle$ as a function of the thermal Stokes number St_θ and various values of St. One clearly observes that when particle inertia increases, the fluctuations of the heat flux become stronger with a maximum deviation from tracers when St_θ is of the order of unity. For the largest Stokes number we have investigated here ($\mathrm{St} = 3.7$), one observes at $\mathrm{St}_\theta = 1$ a gain of a factor almost 3. The variance of the heat flux can be related to the Lagrangian fluid temperature increment. One can indeed easily check, using (3), that statistical stationarity implies

$$\langle \dot{\theta}_p^2 \rangle = \frac{1}{2\tau_\theta^3} \int_0^\infty \langle \delta_\tau \theta^2 \rangle e^{-\tau/\tau_\theta} d\tau, \tag{4}$$

where $\langle \delta_\tau \theta^2 \rangle$ designates the second-order Lagrangian structure function of the fluid temperature along the particle path and over a time lag τ. When $\tau_\theta \ll \tau_\eta$ the integral is concentrated on the small values of τ where the variations of θ are dominated by the δ correlated in time forcing and thus θ diffuses and $\langle \delta_\tau \theta^2 \rangle \sim \tau$. A saddle-point argument then gives $\langle \dot{\theta}_p^2 \rangle \sim \mathrm{St}_\theta^{-1}$ when $\mathrm{St}_\theta \ll 1$, as observed in our data. Conversely, for extremely large τ_θ, the integral is dominated by the large values of τ. When $\tau \gg \tau_L$, one expects $\langle \delta_\tau \theta^2 \rangle \simeq 2\langle \theta^2 \rangle$, so that $\langle \dot{\theta}_p^2 \rangle \sim \mathrm{St}_\theta^{-2}$ for $\tau_\theta \gg \tau_L$, that is $\mathrm{St}_\theta \gg R_\lambda/\sqrt{15}$. In between these two asymptotics, the anomalous scaling $\langle \delta_\tau \theta^2 \rangle \sim \tau^{\zeta_2}$ of the Lagrangian temperature structure function yields a nontrivial behavior. Indeed, when $1 \ll \mathrm{St}_\theta \ll R_\lambda/\sqrt{15}$, the main contribution to the integral comes from τ in the inertial range. This leads to $\langle \dot{\theta}_p^2 \rangle \sim \mathrm{St}_\theta^{\zeta_2 - 2}$, giving a behavior that hence depends on the dynamical Stokes number. The increase of the variance of heat flux as a function of the particle inertia is thus directly related to the enhancement of Lagrangian scalar intermittency. This effect is of course not limited to second-order statistics, as illustrated in the inset of Fig. 5. The probability density functions of $\dot{\theta}_p$ normalized to a unit variance strongly depart from a Gaussian and develop fatter and fatter tails when St increases. This is again a signature of the intermittency of the scalar field sampled by inertial particles.

The clustering of particles in the temperature fronts and the resulting anomalous scaling laws that are found here reveal that a dispersed phase participates in an active and possibly controlled manner to the heat transport in a turbulent flow. Depending on the values of their dynamical and thermal response times, the particles can either act as thermostats or accelerate the diffusion of temperature in the fluid. This can partly explain why heat transfer can be either enhanced or decreased in microdispersed turbulent channel flow, depending on the size of the suspended particles [15]. Such properties can be used to ameliorate and optimize the design of numerous industrial devices ranging from combustion engines to chemical reactors. Furthermore, in addition to thermal properties, the mass transfers between the fluid and the particles are also ruled by the intermittent effects unveiled here. Our results indicate that droplets in turbulent clouds as well as dust particles in protoplanetary disks concentrate at the boundaries between wet and dry, dense and sparse regions. Their inertia allows them to travel across such high-variability zones and thus to experience very different growth histories by condensation or accretion. We expect this effect to be responsible for a critical broadening of the particle size distribution that is not predicted by classical mean-field kinetic approaches. This effect could partly explain the difficulties encountered when estimating the time scales of both rain and planet formation.

This work was performed using HPC resources from GENCI-TGCC (Grant No. 2013-2b6815). The research leading to these results has received funding from the European Research Council under the European Community's 7th Framework Program (FP7/2007-2013, Grant Agreement No. 240579) and from the Agence Nationale de la Recherche (Programme Blanc ANR-12-BS09-011-04).

[1] J. Fan and L. Wang, J. Heat Transfer **133**, 040801 (2011).
[2] W. W. Grabowski and L.-P. Wang, Annu. Rev. Fluid Mech. **45**, 293 (2013).
[3] K. Mann and J. Lazier, *Dynamics of Marine Ecosystems: Biological-Physical Interactions in the Oceans* (John Wiley & Sons, New York, 2009).
[4] A. Johansen, J. S. Oishi, M.-M. Mac Low, H. Klahr, T. Henning, and A. Youdin, Nature (London) **448**, 1022 (2007).
[5] B. I. Shraiman and E. D. Siggia, Nature (London) **405**, 639 (2000).
[6] A. Celani, A. Lanotte, A. Mazzino, and M. Vergassola, Phys. Rev. Lett. **84**, 2385 (2000).
[7] A. Celani, A. Lanotte, A. Mazzino, and M. Vergassola, Phys. Fluids **13**, 1768 (2001).
[8] H. Homann, J. Dreher, and R. Grauer, Comput. Phys. Commun. **177**, 560 (2007).
[9] M. Mathur, G. Haller, T. Peacock, J. E. Ruppert-Felsot, and H. L. Swinney, Phys. Rev. Lett. **98**, 144502 (2007).
[10] S. Goto and J. C. Vassilicos, Phys. Rev. Lett. **100**, 054503 (2008).
[11] M. Maxey, J. Fluid Mech. **174**, 441 (1987).
[12] J. Bec, L. Biferale, M. Cencini, A. Lanotte, S. Musacchio, and F. Toschi, Phys. Rev. Lett. **98**, 084502 (2007).
[13] Y. Sato, E. Deutsch, and O. Simonin, Int. J. Heat Fluid Flow **19**, 187 (1998).
[14] S. Wetchagarun and J. J. Riley, Phys. Fluids **22**, 063301 (2010).
[15] F. Zonta, C. Marchioli, and A. Soldati, Acta Mech. **195**, 305 (2008).